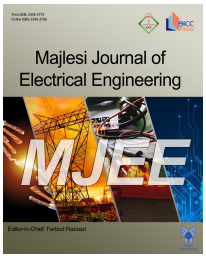

Volume 18, Issue 4, 182452 (1-10)

Majlesi Journal of Electrical Engineering (MJEE)

https://dx.doi.org/10.57647/j.mjee.2024.1804.52

Breakdown characteristics of oxygen and nitrogen gas mixture as substitute gases of sulfur hexafluoride

Norsuhada Zainal Abidin*, Muhammad Saufi Kamarudin, Erwan Sulaiman

Department of Electrical Engineering, Universiti Tun Hussien Onn Malaysia, Parit Raja, Malaysia.

***Corresponding author:** norsuhadazainalabidin@gmail.com

Original Research

Received:
27 April 2024
Revised:
22 June 2024
Accepted:
3 July 2024
Published online:
15 December 2024

Abstract:

Sulfur hexafluoride (SF_6) is extensively used as an essential insulating material in high-voltage industries due to its outstanding electrical characteristics. However, the use of SF_6 gas faces two significant challenges: its substantial impact on global warming and the high toxicity of its breakdown byproducts. This study aims to analyse the breakdown properties of various gas and gas mixtures, including pure Nitrogen (N_2), pure Oxygen(O_2), O_2+N_2 gas mixture, and SF_6+N_2 gas mixture as alternative insulation media under positive standard lightning impulses. The experiments involve sphere and plate electrodes with varying gap distances. Following the BS EN 60060-1 standard, the breakdown voltage is measured using the Up and Down method, with a voltage interval between levels between 1.5% and 3%. Based on the findings, N_2 gas has been determined to be a highly efficient insulator, outperforming other options. This is because of its superior breakdown voltage, which reaches 37.415 kV, and surpasses the values of other gas and gas mixtures.

Keywords: High voltage; Insulator; Alternative; Sulfur hexafluoride

1. Introduction

Climate change poses a substantial peril to the well-being and security of humanity [1]. Climate change impacts both the natural environment and different aspects of human and natural systems, affecting socioeconomic circumstances and the efficiency of health systems [2, 3]. This phenomenon is mainly ascribed to anthropogenic activities that have altered the composition of the Earth's atmosphere in the past few decades. In addition to Carbon Dioxide (CO_2), which makes up about 75% of total emissions and has recently seen a 51% increase, SF_6 is another greenhouse gas primarily produced by human activities. It is an insulating material used in gas-insulated switchgear in the power industry [4, 5]. SF_6 has been widely employed worldwide as an insulating substance in power systems [6–8]. Nevertheless, the extensive utilisation of SF_6 will lead to detrimental environmental consequences, particularly by exacerbating the greenhouse effect. SF_6 gas has a 3,200-year atmospheric life cycle and 23,500 times the Global Warming Potential (GWP) of CO_2 [9, 10]. As a result, it presents a substantial danger to the atmosphere, decreasing its ability to insulate. This occurrence occurs when there is a rise in the lack of uniformity in the electric field, as the electric intensity is crucial in identifying the ideal gas for insulation [11]. Furthermore, the economic feasibility of SF_6 gas is compromised due to its significant demand for Gas Insulated Lines (GIL), resulting in substantial expenses [12]. Due to the difficulties in completely replacing SF_6 in power systems with a single pure gas, binary gas mixtures comprising different types of gases have proven to be a feasible substitute [13]. Throughout the years, continuous efforts have been made to search for substitutes for SF_6 to reduce the use of SF_6 [14, 15].

Three fundamental categories of SF_6 alternatives for gas in technological applications are available. Dry air, CO_2, and N_2 were initially employed in low-voltage switchgear. These gases lack the electrical characteristics needed to miniaturise high-voltage power equipment. Arc extinguishers, such as mixtures SF_6-N_2, are used [16]. This gas insulates, but not as well as SF_6. Thus, it is not the best SF_6 replacement technology. New synthetic gases like carbon

(C), fluorine (F), nitrogen (N), and oxygen (O) make up the third category. These gases C_4F_7N [17–19], $C_5F_{10}O$ [20–22], HFO-1234ze(E) [23, 24], HFO-1336mzz(E) [25–27]. This gas must be mixed with other gases in the power system [23]. Ongoing research is focused on developing an alternative that may not exceed SF_6 in terms of superiority but has similar insulating capacity and is less environmentally harmful. The goal is to evaluate the importance and appropriateness of gas mixtures as insulating materials. The current research effort seeks to further investigate this issue by analysing the breakdown characteristics of gas mixtures when subjected to high-voltage impulses.

The paper outlines the main advantages of discovering breakdown characteristics, including optimising insulation systems. Understanding gas breakdown under diverse situations optimises high-voltage insulating systems. Engineers can build more efficient and dependable insulation systems that handle high voltages by knowing various gases' breakdown voltage and electric field distribution. Selecting appropriate gases is another benefit. Understanding breakdown characteristics helps choose insulating gases or combinations. By investigating gas behaviour under high electric fields, researchers can find environmentally friendly and economically viable replacements to SF_6 with equivalent or better insulating qualities. Understanding breakdown characteristics improves high-voltage system safety. Engineers can design systems with safety margins to minimise unexpected failures and ensure electrical infrastructure reliability by understanding breakdown scenarios. Understanding breakdown characteristics also can enhance high-voltage application performance. Engineers can improve electrical system performance and reliability by optimising gas compositions, electrode designs, and other breakdown parameters to increase breakdown voltages and uniform electric field distributions.

Additionally, researchers can reduce high-voltage insulation's environmental impact by discovering gases with favourable breakdown characteristics. Understanding breakdown characteristics is crucial to replacing SF_6 with environmentally benign alternatives in high electric fields. Overall, finding the breakdown characteristics of gases in high-voltage applications offers numerous advantages, including improved system design, safety, performance, and environmental sustainability.

This paper investigates the behaviour of O_2, N_2, N_2+O_2, and SF_6+N_2 gas mixtures under different electric field profiles. Measuring the electric field at all points between two electrodes is complex, especially in a test chamber with compressed gas and positioned electrodes. Although the method of images by Cloete and van der Merwe can determine the electric field, simulation techniques using electromagnetic software are preferred [8]. The major novelty lies in exploring oxygen O_2 as a component of gas mixtures for high-voltage insulation. N_2 has been intensively explored as a potential alternative to SF_6, however oxygen is rarely added to gas mixtures. The paper introduces O_2 and N_2 in gas mixes and compares their efficacy. This inclusion is unusual since O_2 has different electrical characteristics than N_2 and may present unique advantages or challenges in high-voltage applications. The study provides insight into O_2-N_2 gas mixture breakdown and performance, helping to alternative high-voltage insulation. The breakdown strength of gases under various field utilisation parameters, depending on certain pairs of electrodes, is another significant novelty of this study. This paper compares spherical and planar electrodes and their effects on gas breakdown voltage and electric field distribution. This innovative element provides extensive insights into how electrode shape affects gas breakdown behaviour, optimizing high-voltage insulation systems. The work provides unique insights into gas insulation mechanisms and helps design more efficient and dependable insulation technologies by systematically altering electrode topologies and examining their impacts on breakdown strength.

2. Research methodology

The project commenced with experiments focused on measuring the standard lightning impulse voltage and performing air breakdown tests using plane and sphere electrodes in a high-voltage laboratory. The electrodes are vertical, with the upper electrode linked to the high-voltage terminal and the lower electrode linked to the ground terminal. The primary power source is an alternating current (AC) supply, which is transformed into a direct current (DC) output to generate impulsive voltage using a Silicon Rectifier. The value of 50% of the air's fractional voltage(U_{50}) is determined by applying impulse voltage. The difficulties associated with the electric field are addressed using finite element computer simulation using FEMM software. This approach provides valuable insights into gas testing and the behaviour of electrodes.

2.1 Experimental setup

2.1.1 Configuration for AC high voltage testing

Fig. 1 shows the laboratory arrangement used to generate lightning impulse voltages., conducted across a voltage range of 0 to 220 V. The transformer is engineered to generate high voltage alternating current (AC) from a standard 230 V AC power. It consists of three windings enclosed within an insulating shell. The transformer is equipped with

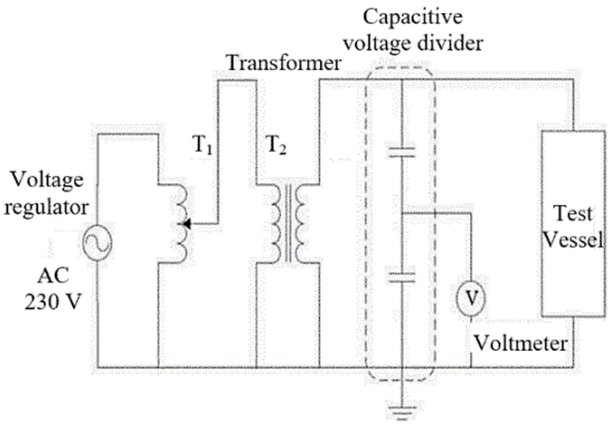

Figure 1. Experimental setup for generation of lightning impulse voltages.

corona-free aluminium shielding electrodes at both the top and bottom for protection. The insulation cylinder is composed of epoxy resin that is strengthened with glass fibre and coated with varnish to avoid the occurrence of tracking. To achieve the necessary impulse voltage for testing purposes, the alternating current (AC) high voltage generated by the transformer will be transformed into direct current (DC) high voltage using a silicon rectifier. This conversion aims to obtain a high voltage for impulse voltage testing by using direct current (DC). Fig. 2 shows the experimental setup for this project.

The experiment employs a transformer that operates at a frequency of 50 Hz and is equipped with a coupling winding for an avalanche connection. This transformer can deliver high voltage alternating current of up to 100 kV. AC voltage measurement is conducted by employing a capacitive divider with a capacitance of 100 pF. The test configuration is linked to a pressure vessel housing the studied gas.

The controlled test environment minimizes the influence of external factors on experimental results. External factors such as temperature fluctuations, humidity, and electromagnetic interference are carefully mitigated to ensure the reliability and reproducibility of measurements. The experiments can accurately assess the intrinsic breakdown characteristics of gases without interference from external variables by maintaining consistent pressure, temperature, and electrical parameters within the pressure vessels. The absence of external factors enhances the accuracy and validity of experimental results, allowing researchers to draw meaningful conclusions about the performance of gases as insulators under high-voltage conditions. Overall, the controlled test environment ensures that the experiments are conducted under precise and reproducible conditions to evaluate the breakdown characteristics of gases and their suitability for high-voltage insulation applications.

2.1.2 Design and operation of gas pressure vessels

A minimum thickness of 10 millimetres (mm)is applied to the vessel's top, bottom, and side walls in this configuration. This design intends to minimise the amount of gas needed for each test. Fig. 3 shows the pressure vessel of this experiment. The vessel is comprised of a Plexiglass cylinder surrounded by both upper and bottom rims connected to high voltage and ground through an electrical connection. The upper and lower flanges are fitted with a vacuum gauge, pressure gauge, and inlet and outlet valves.

Figure 2. Experimental setup.

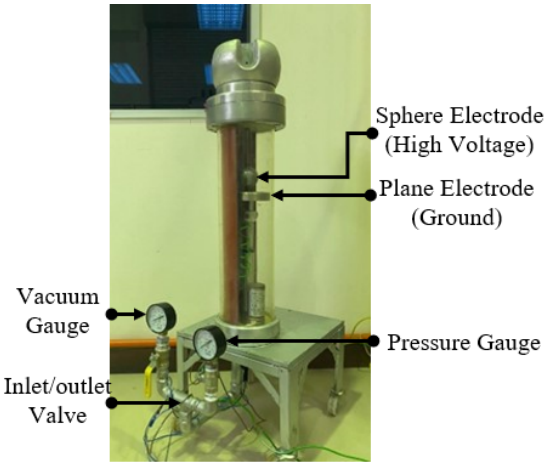

Figure 3. Pressure vessel.

The electrodes can be modified or substituted by detaching the upper and lower plates of the container. The vessel has dimensions of 60 cm in height and 12 cm in width, with a volume of 67.85 litres. The top bushing conductor of the vessel is connected to a high-voltage supply, while the bottom conductor is connected to the ground. The transparent design facilitates observations during the testing of gas.

The experimental configuration employs two sets of gauges to ensure precise pressure measurement. A -1 to $+1$ bar gauge is utilised to measure pressures below 1 bar (absolute), whereas a distinct gauge is employed for measuring pressures over 1 bar. The selected gauges have a 100 mm diameter and a 16.7 mm bottom entry, ensuring a smooth transition between vacuum and pressurised conditions. This improves the accuracy of pressure readings. The experiments are conducted within pressure vessels designed to maintain a controlled environment for gas testing. These vessels are constructed with specific materials and dimensions to withstand high pressures and minimize gas leakage.

2.1.3 Electrode configurations

The electrodes used in the experiments are precisely designed and positioned within the pressure vessels to create uniform electric fields and facilitate accurate measurements. Different electrode configurations, such as spherical and planar electrodes, are utilized to study their effects on breakdown characteristics. Various factors, including the presence of tiny protrusions on the surfaces of the electrodes, influence the breakdown voltage. Generally, the breakdown voltage will increase in direct proportion to the smoothness of the surface finish.

In this study, the electrode options consist of a spherical electrode with a radius of 5.0 cm and a planar electrode with a radius of 1.0 cm. Fig. 4 shows the electrode setup of the project. The electrodes inside the vessel have a consistent threaded dimension that matches the bushing, guaranteeing a tight and stable connection. The high-voltage electrodes

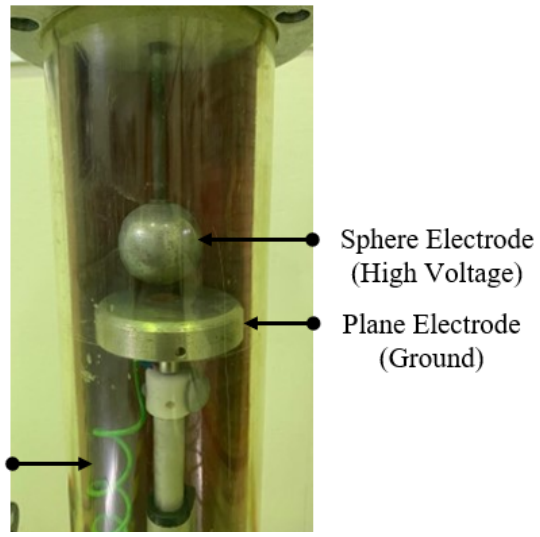

Figure 4. Electrode Set Up.

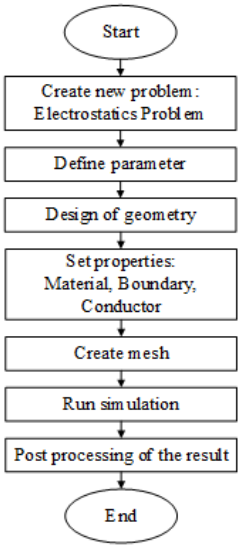

Figure 6. Flowchart of the simulation.

are firmly attached to the bushing and do not move, while the ground electrodes can shift in position.

2.1.4 Simulation study by using FEMM software

This project simulated and generated electrostatic problem results using FEMM software. FEMM simulation relies on the electrostatic pre- and post-processors. The pre-processor creates geometry sketches, specifies materials, and sets boundary constraints. The post-processor generates outputs and visualises the solution. Accurate results require appropriate parameter selection. After finding the U_{50}, the FEMM software finds the electrode's electrical stress or maximum electric field strength (Emax). Emax refers to the highest level of electric field intensity that a material can endure without experiencing dielectric breakdown [28]. Fig. 5 shows the sphere-to-plane electrode configuration designed by using FEMM software. An electrostatic problem is used to study electric field strength, E, and flux density. At the same time, Fig. 6 shows the flowchart of the simulation software FEMM, which is utilised to obtain the Emax. The 'Axisymmetric' type ensures that the simulated sphere and plane electrodes exhibit symmetry along a specific axis, usually the z-axis. This implies that the system can rotate about this axis without causing any changes to its general shape or characteristics.

The names of the material, boundary, and conductor properties have been changed to streamline the review process. A mesh is needed to break an electrostatic problem's geometry into smaller components to ensure the precision of electrostatic field equations. Then, the program can determine the highest field intensity.

3. Results and discussion

The primary findings of this study involve two aspects: the acquisition of U_{50} by experimental work and the determination of the field utilisation factor using simulation on FEMM software. Fig. 7 displays the field intensity of electric field zones, represented by colour according to the simulation findings. Finite Element Magnetic Method (FEMM) soft-

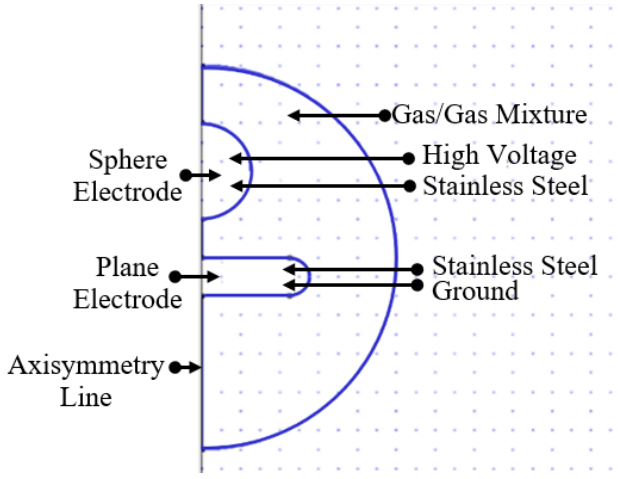

Figure 5. Sphere-to-plane electrode configuration.

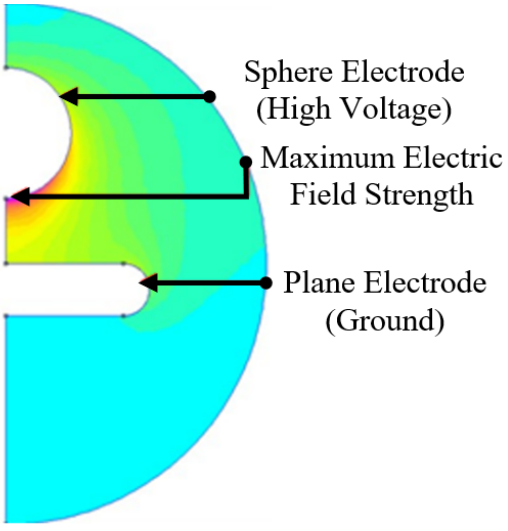

Figure 7. Maximum electric field at FEMM.

ware is employed for simulation studies to complement experimental results. This software allows for the modeling and calculating electric field distributions under various conditions, providing additional insights into gas breakdown characteristics.

3.1 Pure nitrogen

Fig. 8 illustrates the relationship between U_{50} and the gap length for pure N_2. By analysing the results, the value of U_{50} increases as the gap length increases. Certainly, the gas demonstrates superior resilience to high voltage when subjected to a sphere-plane electrode configuration. The relationship between Emax and electrical breakdown is crucial in assessing the dependability of the high-voltage-ground electrode configuration.
Fig. 9 shows the Emax, and Fig. 10 shows the electric field utilization factor. Table 1 displays the field utilisation factor (η) for pure N_2. To determine the electric field utilisation factor (η), the average electric field (Eav) is divided by the maximum electric field (Emax). Fig. 10 demonstrates a clear inverse relationship in which the field utilisation factor falls as the gap grows. A greater field utilisation factor indicates a more evenly distributed field configuration. Varying the gap length between electrodes will result in

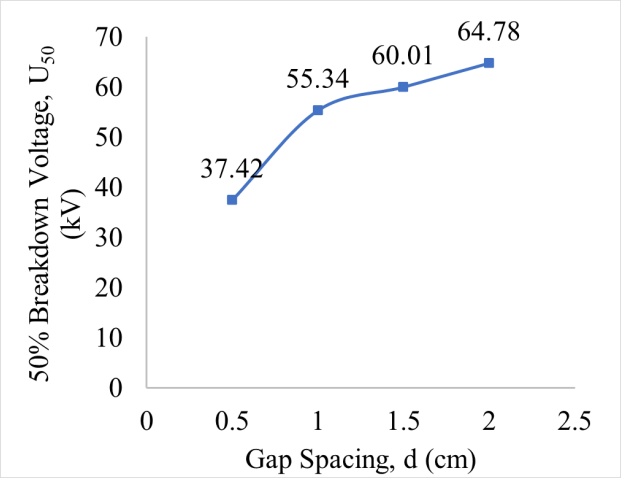

Figure 8. U_{50}(kV) against d (cm) for pure N_2 gas.

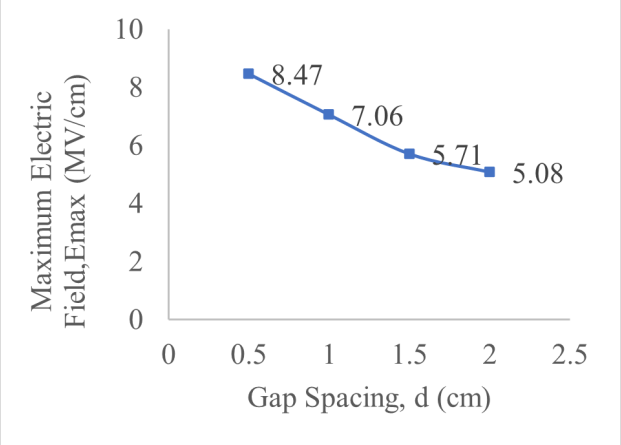

Figure 9. Emax versus distance, d for N_2 gas.

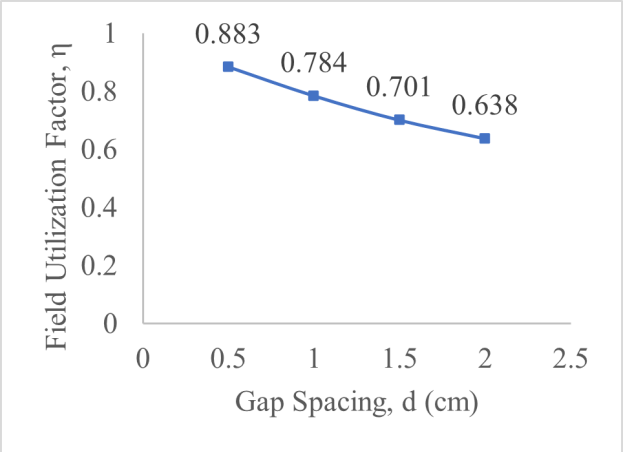

Figure 10. Field utilization factor against gap distance for N_2 gas.

Table 1. The pure N_2 gas mixture field utilisation factor (η).

Electrode Gap, d (cm)	50% Breakdown Voltage, U_{50} (kV)	Emax (MV/cm)	Field Utilization Factor, η
0.5	37.42	8.47	0.883
1.0	55.34	7.06	0.784
1.5	60.01	5.71	0.701
2.0	64.78	5.08	0.638

different breakdown voltages. When the space between the electrodes is increased, the intensity of the electric field that exists between the electrodes diminishes. This suggests that a greater voltage is required to get the gas to undergo breakdown.

3.2 Pure oxygen

According to the calculation, the U_{50} values increase as the gap spacing widens, with various rates of increase. This is shown in Table 2 and Fig. 11. The most significant rise in 50% breakdown voltage values is observed specifically between gap spacings of 0.5 cm and 1.0 cm, compared to other gap distances. The values of the field utilization factor are presented in Table 2. Fig. 12 shows the E_{max} for pure O_2. A larger gap results in a lower field utilisation factor, as depicted in Fig. 13. These findings indicate that a gap distance of 0.5 cm results in a more consistent electrode configuration. The field utilisation factor is the same for each gap distance in any gas insulator in this study. Increas-

Table 2. The pure O_2 field utilisation factor (η).

Electrode Gap, d (cm)	50% Breakdown Voltage, U_{50} (kV)	Emax (MV/cm)	Field Utilization Factor, η
0.5	34.12	7.72	0.884
1.0	57.83	7.38	0.784
1.5	66.55	6.33	0.701
2.0	75.82	5.94	0.638

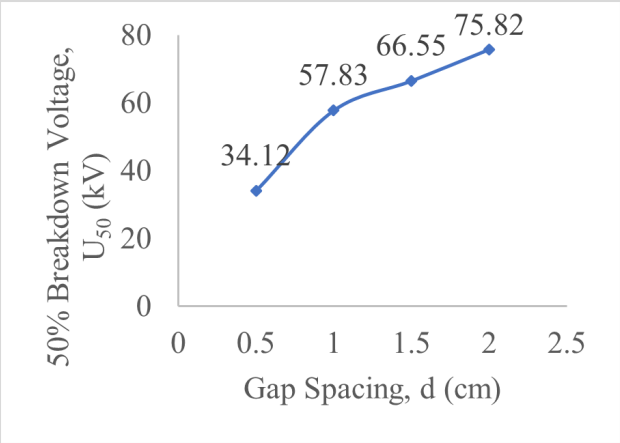

Figure 11. U_{50}(kV) against d for pure O_2 gas.

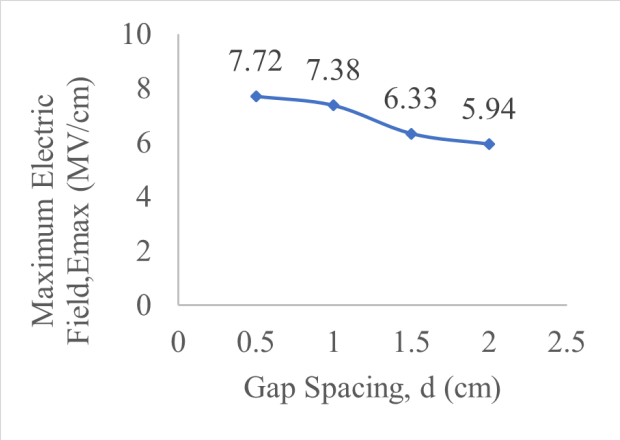

Figure 12. E_{max} versus distance, d for O_2 gas.

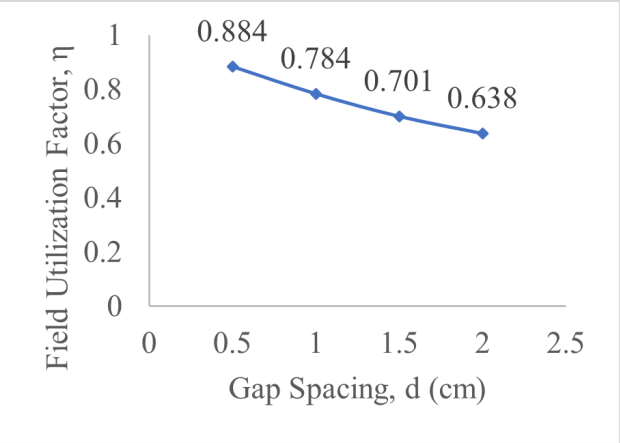

Figure 13. Field utilization factor against gap distance for O_2 gas.

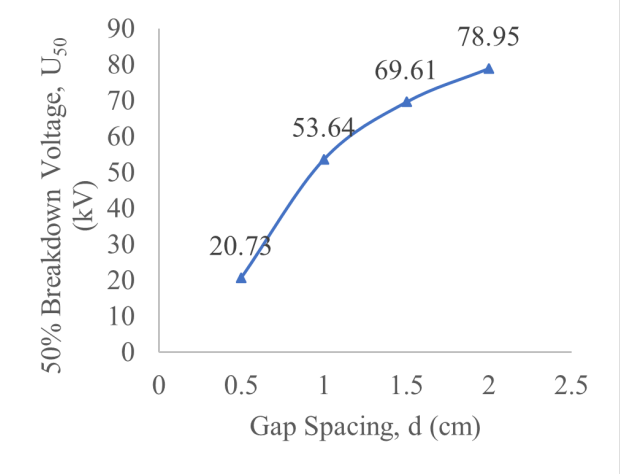

Figure 14. U_{50}(kV) against d(cm) for O_2 and N_2 gas mixture.

ing the gap spacing will result in a decrease in value, so achieving the intended outcome. The field utilisation factor is unaffected by the selection of gas as an insulator, but the arrangement of the electrodes influences it. The simulation in FEMM software demonstrates that each electrode arrangement has a unique electric field distribution.

3.3 Nitrogen and oxygen gas mixture

Based on the calculation and Fig. 14, the U_{50} values demonstrate varying rates of increase as the gap spacing widens. The increase in breakdown voltage by 50% when the gap spacing is increased from 0.5 cm to 1.0 cm is the most notable compared to other gap spacings, as shown in Table 3. Fig. 15 shows Emax for the O_2 and N_2 gas mixture. The field utilisation factor diminishes as the gap distance increases, as depicted in Fig. 16. A research investigation was carried out to analyse the behaviour of Hexafluorobutene ($C_4H_2F_6$) gas, both on its own and when mixed with CO_2 and N_2, using different electrode configurations [29]. The study determined that with an air gap of 0.6 cm, the field utilisation factor for sphere-to-plane electrode configurations was 0.74. This indicates that the data obtained from this research were considered credible. The data obtained from this study suggests that using a gap distance of 0.5 cm leads to a more uniform electrode arrangement.

Table 3. The O_2 and N_2 gas mixture field utilisation factor (η).

Electrode Gap, d (cm)	50% Breakdown Voltage, U_{50} (kV)	Emax (MV/cm)	Field Utilization Factor, η
0.5	20.73	4.69	0.884
1.0	53.64	6.85	0.783
1.5	69.61	6.62	0.701
2.0	78.95	6.19	0.638

3.4 SF_6 and N_2 gas mixture

Nitrogen, acknowledged for its exceptional stability, inertness, and abundant availability, is considered an essential additive to SF_6. Introducing 50% SF_6 into nitrogen results in a notable enhancement of the breakdown strength.
Table 4 shows that U_{50} increases as the gap distance widens. The increase in U_{50} during a positive impulse is substantial. However, the disparity in U_{50} values for each gap increment decreases. The breakdown voltage is 20.11 kV for 0.5 cm to 1.0 cm, 17.89 kV for 1.0 cm to 1.5 cm, and 15.38 kV for 1.5 cm to 2.0 cm. The electric field strength positively

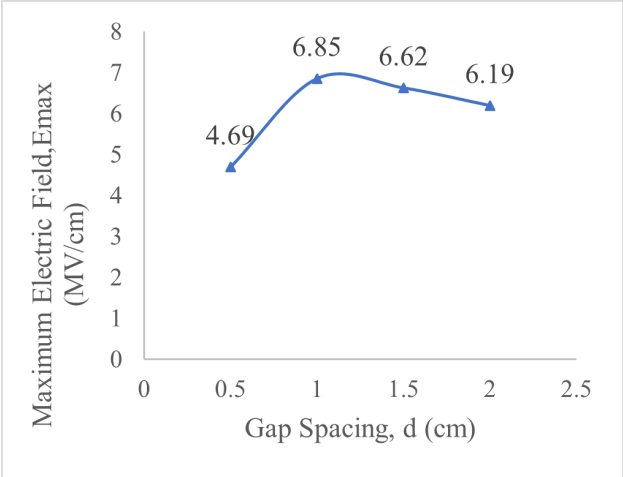

Figure 15. Emax versus distance, d for O_2 and N_2 gas mixture.

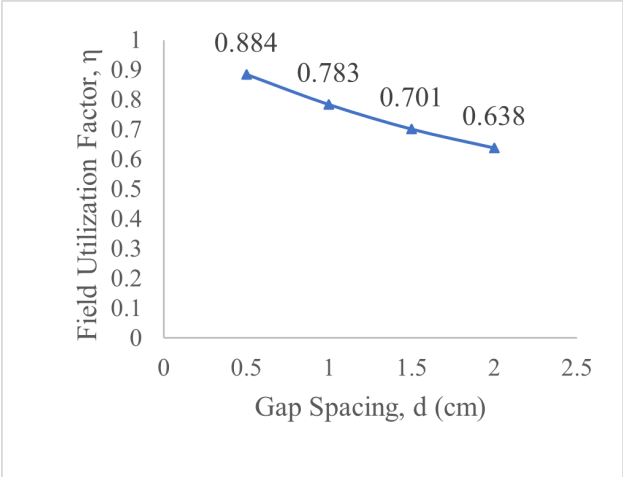

Figure 16. Field utilization factor against gap distance for O_2 and N_2 gas mixture.

Table 4. The SF_6 and N_2 gas mixture field utilisation factor (η).

Electrode Gap, d (cm)	50% Breakdown Voltage, U_{50} (kV)	Emax (MV/cm)	Field Utilization Factor, η
0.5	32.58	1.73	0.038
1.0	59.06	2.78	0.034
1.5	81.50	3.70	0.015
2.0	88.74	4.00	0.011

correlates with SF_6 and N_2 gas mixture U_{50} at 0.5 cm. The variation in electric field magnitude for each gap distance corresponds to a positive surge, as spark discharges tend to happen earlier in the trailing portion of the lightning surge waveform during a positive surge. As a result, when the distance between the electrodes increases, the U_{50} and the E_{max} increase, as shown in Fig. 17 and Fig. 18. Nevertheless, the field utilization factor diminishes as the gap length increases, as illustrated in Fig. 19.

A study conducted on Perfluoroisobutyronitrile (C_4F_7N) ex-

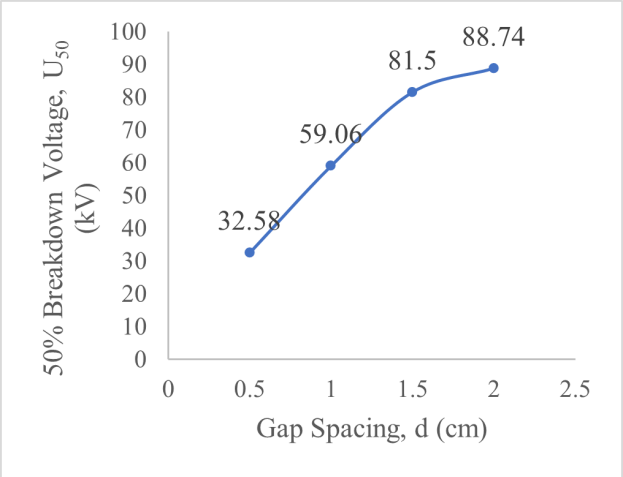

Figure 17. U_{50}(kV) against d(cm) for SF_6 and N_2 gas mixture.

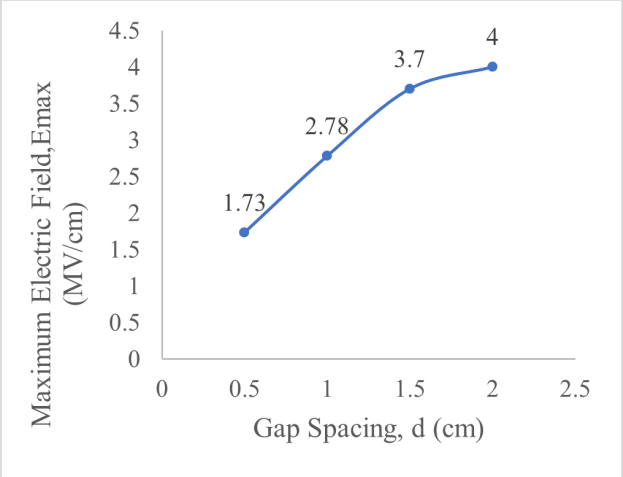

Figure 18. E_{max} versus distance, d for SF_6 and N_2 gas mixture.

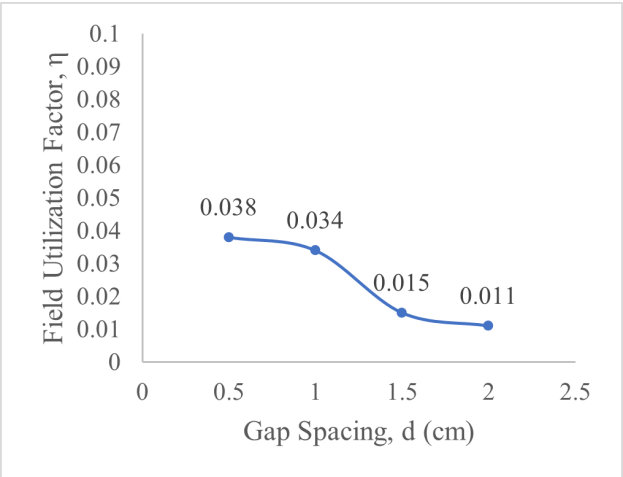

Figure 19. Field utilization factor against gap distance for SF_6 and N_2 gas mixture.

amined its behaviour under various electrode configurations [30]. The study determined that the Emax for sphere-to-

sphere electrode configurations was 1.785 MV when the air gap between the electrodes was 0.5 cm. The results acquired by this research were deemed reliable. Nitrogen gas is an inert gas that has a high collision cross-section. N_2 in SF_6 would cause electron-N_2 collisions that are rigid. SF_6 molecules might absorb electrons if stimulated, and their energy is lowered. SF_6 gas molecules can absorb many low-energy electrons during a positive lightning impulse. As SF_6 content rises, more molecules absorb electrons and create negative ions, increasing breakdown voltage. After a certain concentration of SF_6, the number of low-energy electrons diminishes, preventing SF_6 molecules from absorbing electrons and forming negative ions. Thus, increasing SF_6 concentration to increase breakdown voltage is pointless. Initial electrons' speed and energy prohibit them from absorbing fewer low-energy electrons during a negative lightning impulse. The breakdown voltage will reach saturation quickly with more SF_6 and a negative lightning impulse.

4. Conclusion

SF_6 exhibits exceptional dielectric characteristics, yet a prolonged atmosphere lifespan and a substantial global warming potential burden it. The limitations of these drawbacks have restricted its usage. Hence, it is imperative to implement a proficient and ecologically sustainable substitute. Nitrogen gas was highly efficient as an insulator compared to oxygen gas, mixtures of nitrogen and oxygen gases, and mixtures of sulfur hexafluoride and nitrogen gases. N_2 gas is the most popular and least expensive electropositive gaseous dielectric. Positive ions are formed when electropositive gas molecules attempt to give up electrons. According to the previously discussed results, the breakdown characteristics of the four types of gas insulators did not differ significantly, given the consistent pressure applied in this study. To examine insulation properties more precisely, various pressure conditions must be applied.

Acknowledgement
This research was supported by Universiti Tun Hussein Onn Malaysia (UTHM) through GPPS (vot Q321) and Tier 1 (vot Q352).

Authors contributions
All authors have contributed equally to prepare the paper.

Availability of data and materials
The data that support the findings of this study are available from the corresponding author upon reasonable request.

Conflict of interests
The authors declare that they have no known competing financial interests or personal relationships that could have appeared to influence the work reported in this paper.

References

[1] S. Shi et al. "**Recent advances in degradation of the most potent industrial greenhouse gas sulfur hexafluoride**.". *Elsevier BV*, 15, 2023. DOI: https://doi.org/10.1016/j.cej.2023.144166.

[2] World Health Organization. "**Climate change," World Health Organization**.". *Accessed*, 24, 2023.

[3] K. Abbass, M. Z. Qasim, H. Song, M. Murshed, H. Mahmood, and I. Younis. "**A review of the global climate change impacts, adaptation, and sustainable mitigation measures**.". *Environmental Science and Pollution Research*, 29(28):pp. 42539–42559, 2022. DOI: https://doi.org/10.1007/s11356-022-19718-6.

[4] A. Hopf, M. Rossner, F. Berger, and U. Prucker. "**Dielectric strength of alternative insulation gases at high pressure in the homogeneous electric field**.". *Electrical Insulation Conference (EIC)*, 2015. DOI: https://doi.org/10.1109/ICACACT.2014.7223575.

[5] M. An et al. "**Sustained growth of sulfur hexafluoride emissions in China inferred from atmospheric observations**.". *Nat Commun*, 15(1), 2024. DOI: https://doi.org/10.1038/s41467-024-46084-3.

[6] B. Boychev. "**Comparison of SF_6 alternative gases**.". *14th Electrical Engineering Faculty Conference*, 2022. DOI: https://doi.org/10.1109/BulEF56479.2022.10021206.

[7] Z. Yang, Y. Li, Y. Wang, X. Zhang, K. Wan, and Y. Zhang. "**Experimental study on the effect of H_2 on the degradation of SF_6 by pulsed dielectric barrier discharge**.". *IEEE Transactions on Dielectrics and Electrical Insulation*, 31(1):pp. 448–456, 2024. DOI: https://doi.org/10.1109/TDEI.2023.3301828.

[8] L. Bellofatto, P. Sigismondi, and I. S. P. A. Imesa. "**SF_6 free alternative-study of ternary mix natural gas for electrical insulation purpose**.". *PCIC Energy Europe (PCIC Energy)*, 2023.

[9] J. Owens, A. Zhang, J. Bonk, and M. Delorme. "**Review of health and safety data on leading SF_6-alternative gas mixtures**.". *IEEE International Conference on High Voltage Engineering and Applications, ICHVE*, 2022. DOI: https://doi.org/10.1109/ICHVE53725.2022.10014453.

[10] S. Tian et al. "**Study on subacute inhalation toxicity and offspring teratogenicity of C_4F_7N: An environmentally friendly insulating gas to replace SF_6**.". *J Clean Prod*, 387, 2023. DOI: https://doi.org/10.1016/j.jclepro.2022.135799.

[11] C. Guo et al. "**Influence of electric field non-uniformity on breakdown characteristics in SF_6/N_2 gas mixtures under lightning impulse**.". *IEEE Transactions on Dielectrics and Electrical Insulation*, pages pp. 2248–2258, 2017. DOI: https://doi.org/10.1109/TDEI.2017.006261.

[12] P. Boffi, A. Iadanza, and M. Mammeri. "**Sustainability through SF_6 reduction on HV/E-HV cable accessories**.". *AEIT International Annual Conference (AEIT)*, pages pp. 1–5, 2022. DOI: https://doi.org/10.23919/AEIT56783.2022.9951823.

[13] S. Xiao, X. Zhang, J. Tang, and S. Liu. "**A review on SF_6 substitute gases and research status of CF3I gases**.". *Energy Reports*, 4:pp. 486–496, 2018. DOI: https://doi.org/10.1016/j.egyr.2018.07.006.

[14] G.V. Kumar, R. Verma, G. Singh, M.K. Warrier, and A. Sharma. "**An experimental and numerical study: to investigate the switching characteristics of a field-distortion sparkgap switch in various SF_6 admixtures**.". *Engineering Research Express*, 5(4), 2023. DOI: https://doi.org/10.1088/2631-8695/ad0fc2.

[15] H. Lee, J. Yeun, H. Ahn, J. Choi, and Y. Kim. "**Insulation design of 25.8kV class gas insulated switchgear in Dry Air**.". *ICEPE-ST 2022 - 6th International Conference on Electric Power Equipment - Switching Technology*, pages pp. 253–256, 2022. URL 10.1109/ICEPE-ST51904.2022.9757091.

[16] L. Wang, X. Wen, Y. Wang, and J. Zhao. "**Research about insulation characteristic of $SF_6/CO_2/N_2$ and $CF_3I/CO_2/N_2$ gas mixtures at different proportions**.". *ICPET*, pages pp. 236–241, 2022. DOI: https://doi.org/10.1109/ICPET55165.2022.9918480.

[17] R. Ahmed, R. A. Rahman, M. S. Kamarudin, M. F. M. Yousof, H. B. Ahmad, and A. A. Salem. "**Feasibility of fluoronitrile (C_4F_7N) as a substitute to sulphur hexafluoride (SF_6) in gas insulated application: A review**.". *IEEE International Conference on Power and Energy*, pages pp. 391–396, 2022. DOI: https://doi.org/10.1109/PECon54459.2022.9988941.

[18] Y. Meng, Z. Li, H. Xue, W. Ding, Z. Deng, and W. Liu. "**Surface flashover characteristics of the 252-kV Conical insulator in C_4F_7N/CO_2 gas mixture**.". *IEEE Transactions on Dielectrics and Electrical Insulation*, 30(2):pp. 717–725, 2023. DOI: https://doi.org/10.1109/TDEI.2023.3249653.

[19] J. Y. Na, R. Hwang, S. J. Cho, T. H. Song, and B. W. Lee. "**Breakdown characteristics of a fluoronitrile mixture gas according to mixing ratio and oxygen content for high-voltage power equipment application**.". *IEEE Access*, 12:pp. 16117–16126, 2024. DOI: https://doi.org/10.1109/ACCESS.2024.3359304.

[20] D. Su et al. "**Experimental research on V-t characteristics of $C_5F_{10}O/CO_2$ gas mixture under lighting impulse voltage**.". *IEEE Transactions on Dielectrics and Electrical Insulation*, 30(5):pp. 2134–2141, 2023. DOI: https://doi.org/10.1109/TDEI.2023.3276336.

[21] F. Zeng et al. "**Switching impulse characteristics of $C_5F_{10}O$ gas mixtures under extremely nonuniform field**.". *IEEE Transactions on Dielectrics and Electrical Insulation*, 29(4):pp. 1617–1624, 2022. DOI: https://doi.org/10.1109/TDEI.2022.3185582.

[22] F. Zeng et al. "**Breakdown characteristics of eco-friendly gas $C_5F_{10}O/CO_2$ under switching impulse in nonuniform electric field**.". *IEEE Transactions on Dielectrics and Electrical Insulation*, 29(3):pp. 866–873, 2022. DOI: https://doi.org/10.1109/TDEI.2022.3168334.

[23] N. Tang, K. Wang, Y. Yao, B. Zhang, and X. Li. "**Dielectric properties of HFO-1336mzz(E)/N_2 mixture as a possible SF_6-substitute gas**.". *IEEE International Conference on High Voltage Engineering and Applications, ICHVE*, 2022. DOI: https://doi.org/10.1109/ICHVE53725.2022.10014483.

[24] P. Ranjan et al. "**Lightning impulse and AC breakdown characteristics of SF_6 and its alternatives**.". *IEEE 2022 4th International Conference on Dielectrics, Proceedings*, pages pp. 672–675, 2022. DOI: https://doi.org/10.1109/ICD53806.2022.9863486.

[25] J. Liu et al. "**Negative DC dielectric breakdown characteristics and synergistic effect of HFO-1336mzz(E) mixtures**.". *IEEE Transactions on Dielectrics and Electrical Insulation*, 30(1):pp. 65–73, 2023. DOI: https://doi.org/10.1109/TDEI.2022.3214166.

[26] B. Zhang, K. Wang, Y. Yao, K. Li, X. Li, and N. Tang. "**Insulation characteristics of HFO-1336mzz(E) and its mixtures as eco-friendly alternatives to $SF_6$for medium-voltage switchgears**.". *IEEE Transactions on Dielectrics and Electrical Insulation*, 30(2):pp. 536–545, 2023. DOI: https://doi.org/10.1109/TDEI.2023.3249652.

[27] F. Wang et al. "**Surface flashover characteristics of epoxy Resin in HFO-1336mzz(E)/CO_2 gas mixtures under negative DC voltage**.". *IEEE Transactions on Dielectrics and Electrical Insulation*, 30(5):pp. 2067–2074, 2023. DOI: https://doi.org/10.1109/TDEI.2023.3298758.

[28] H. Palneedi, M. Peddigari, A. Upadhyay, J. P. B. Silva, G. T. Hwang, and J. Ryu. "**Lead-based and lead-free ferroelectric ceramic capacitors for electrical energy storage**.". *Ferroelectric Materials for Energy Harvesting and Storage, Elsevier*, pages pp. 279–356, 2020. DOI: https://doi.org/10.1016/B978-0-08-102802-5.00009-1.

[29] R. Ahmed, R. A. Rahman, A. S. Aldosary, B. Al-Ramadan, R. Ullah, and A. Jamal. "**Analysis of the insulation characteristics of hexafluorobutene ($C_4H_2F_6$) gas and mixture with CO_2/N_2 as an alternative to SF_6 for medium-voltage applications**.". *Applied Sciences*, 13(5), 2023. DOI: https://doi.org/10.3390/app13158940.

[30] R. Ahmed, R. A. Rahman, N. Najihah, and A. Latif. "**Characterization of electric field profile for C_4F_7N with CO_2 under different electrode configurations**.". *Evolution in Electrical and Electronic Engineering*, 3(1):pp. 587–597, 2022. DOI: https://doi.org/10.30880/eeee.2022.03.01.068.